Geophysical Research Letters

RESEARCH LETTER
10.1029/2022GL102548

Influence of Organized Turbulence on OH Reactivity at a Deciduous Forest

Olivia E. Clifton[1,2], Edward G. Patton[1], Mary Barth[1], John Orlando[1], Siyuan Wang[3], and Colleen Baublitz[4,5,6]

[1]National Center for Atmospheric Research, Boulder, CO, USA, [2]Now at NASA Goddard Institute for Space Studies, NY, NY, USA, [3]NOAA Chemical Sciences Laboratory, Boulder, CO, USA, [4]Department of Earth and Environmental Sciences, Columbia University, Palisades, NY, USA, [5]Lamont-Doherty Earth Observatory, Columbia University, Palisades, NY, USA, [6]Now at Office of Research and Development, US Environmental Protection Agency, Research Triangle Park, NC, USA

Key Points:

- Turbulence-induced segregation between hydroxyl radical (OH) and isoprene in the forest canopy changes strongly with height, soil NO emissions, and sunlight
- At the height of the maximum impact inside the canopy, OH-isoprene segregation can alter the OH reactivity by −9% to +1%
- There may be differences in bottom-up estimates and direct measurements of OH reactivity due to segregation (up to 3%–4% at canopy top)

Supporting Information:

Supporting Information may be found in the online version of this article.

Correspondence to:

O. E. Clifton,
olivia.e.clifton@nasa.gov

Citation:

Clifton, O. E., Patton, E. G., Barth, M., Orlando, J., Wang, S., & Baublitz, C. (2023). Influence of organized turbulence on OH reactivity at a deciduous forest. *Geophysical Research Letters*, *50*, e2022GL102548. https://doi.org/10.1029/2022GL102548

Received 16 DEC 2022
Accepted 11 MAR 2023

Abstract Oxidation of reactive carbon fuels climate- and pollution-relevant chemistry. Deciduous forests are important sources of reactive carbon (particularly isoprene). Organization in turbulence can physically separate ("segregate") oxidants from reactive carbon, causing oxidation to increase or decrease relative to the (ubiquitous) assumption of well-mixed conditions. We use large eddy simulation coupled to a multilayer canopy model and simplified chemistry to quantify the impact of segregation on near-canopy hydroxyl radical (OH) reactivity. Simulations mimic summer clear-sky midday and morning conditions at a homogeneous deciduous forest. OH-isoprene segregation alters OH reactivity inside the canopy by up to 9%, but the impact strongly depends on height, soil NO emissions, and sunlight. Uniquely, we identify the drivers of changes by isolating the roles of isoprene and OH. Our findings also suggest that segregation may create discrepancies between direct measurements and bottom-up estimates of OH reactivity, separate from the issue of mischaracterized or unknown OH sinks.

Plain Language Summary Forests are a large source of chemically reactive carbon-containing gases to the atmosphere. Oxidation of these gases influences air quality and climate. The air motions that transport the gases out of forest canopies are structured or organized in a particularly unique way. These structured air motions can also physically separate compounds that may otherwise react with each other in canopy air spaces, especially because there are natural and dynamic chemical sources and sinks in canopies that are also influenced by the structured air motions. Here we use a computer model with very high resolution to show that accounting for the physical separation of a primary carbon-containing compound emitted by leaves and a key oxidant between the organized motions can accelerate or decelerate the atmospheric chemical reactivity calculated with the widely used assumption of well-mixed conditions, with the sign and magnitude of the impact depending on the environmental and chemical conditions.

1. Introduction

The hydroxyl radical (OH) is the most important atmospheric oxidant, critical to the formation and destruction of many greenhouse gases and toxic air pollutants. OH reacts quickly with many compounds, challenging accurate OH measurements and predictive ability. Constraints on OH reactivity (OH_r) are key to better understanding of OH. Organized turbulence in the atmospheric boundary layer (ABL) may physically separate ("segregate") OH from the compounds with which it reacts. Starting with Krol et al. (2000), a series of papers have suggested nonnegligible (e.g., 10%–40%) segregation of OH with its reactants (e.g., Butler et al., 2008; Dlugi et al., 2010; Kim et al., 2016; Patton et al., 2001). If segregation between OH and reactants is nonnegligible, then OH_r can be either slower or faster than the OH_r estimated with the (ubiquitous) assumption of well-mixed conditions. Many papers examine segregation between OH and reactants, but to our knowledge only Brosse et al. (2018) examine segregation's impact on OH_r, focusing on the influence of moist thermals in different chemical regimes. Here we also investigate segregation impacts on OH_r and changes with chemical regimes, but under very different environmental and chemical conditions and with a focus on the forest canopy.

Isoprene is emitted by vegetation, and deciduous forests are a large source of isoprene and thus oxidized reactive carbon that can lead to ozone and secondary organic aerosol formation (Carlton et al., 2009; Chameides et al., 1988; Guenther et al., 1995, 2012; Trainer et al., 1987). Previous work examines segregation between

isoprene and OH using a variety of approaches (Brosse et al., 2018; Butler et al., 2008; Dlugi et al., 2010; Karl et al., 2007; Kaser et al., 2015; Kim et al., 2016; Krol et al., 2000; Li, Y. et al., 2016; Ouwersloot et al., 2011), in many cases probing the impact of clouds and land surface heterogeneity, which create large-scale organization in mixed-layer turbulence and isoprene emissions. Notably, segregation can also be important inside and right above forest canopies due to the combination of distinct organization in turbulent air motions and dynamic reactant sources and sinks that vary with height in the canopy, even across homogenous landscapes and under clear sky conditions (Clifton et al., 2022; Edburg et al., 2012; Patton et al., 2001). Specifically, in this work, we probe the impact of near-canopy isoprene-OH segregation on OH_r under clear-sky conditions at a homogeneous forest by leveraging a new version of the NCAR large eddy simulation (LES) coupled to a multilayer canopy model that simulates the broad range of scales contributing to organized turbulence over and inside canopies (Patton et al., 2016) as well as chemistry and interactive leaf-level chemical sources and sinks (Clifton et al., 2022).

Nitrogen oxides ($NO_x = NO + NO_2$) influence oxidation because NO_x is a source and sink of HO_x ($=OH + HO_2$). One study finds that ABL OH-isoprene segregation strongly depends on NO_x (Kim et al., 2016). The authors attribute stronger segregation with lower NO_x to lower OH and thus higher isoprene and stronger variability (Kim et al., 2016). Another study finds a minimal impact of an order-of-magnitude change in soil NO emissions (originally 0.5 ppt m s^{-1}) on ABL OH-isoprene segregation, but a factor of 1.6–1.7 increase with free tropospheric NO_2 increasing from 0 to 0.5 ppb (Ouwersloot et al., 2011). Only Clifton et al. (2022) examine the role of NO_x on segregation in the vicinity of the forest canopy, showing differences with upper versus lower bounds on soil NO (Li et al., 2007; Thornton et al., 1997; Williams & Fehsenfeld, 1991). In Clifton et al. (2022), we use spectral analysis to tease apart the causes of differences of segregation of NO_x-containing reactions with increases in soil NO emissions. In general, however, prior work barely scratches the surface in terms of understanding rather than simply identifying segregation changes with environmental and chemical conditions. In the work presented here, we build on Clifton et al. (2022) by examining OH-isoprene segregation's impact on OH_r and further investigating changes with soil NO emissions, additionally including a simulation with very high soil NO emissions. Specifically, we isolate the roles of individual variations in isoprene and OH versus co-variations in the two quantities by examining their average correlations and individual standard deviations, as well as using spectral analysis to identify how the relationship between OH and isoprene changes on different temporal/spatial scales. We also introduce a new set of the soil NO simulations to test the effects of sunlight (e.g., changes in photochemistry, turbulence, isoprene emissions)—perturbing an environmental condition not yet examined for which we find strong changes in segregation within the canopy.

2. Model Configuration and Simulations

The NCAR-LES (e.g., Moeng, 1984; Moeng & Wyngaard, 1988; Sullivan et al., 1996; Sullivan & Patton, 2011) has been coupled to a multilayer canopy model (MLM) for a homogeneous temperate deciduous forest and summer clear-sky conditions (Clifton & Patton, 2021; Patton et al., 2016). The model domain is 2,048 m in the horizontal directions and 1,024 m in the vertical direction with 2-m resolution. There are vertical changes in light attenuation. Height-varying canopy moisture and heat sources and sinks as well as canopy drag respond to local atmospheric variations and influence turbulent flow (Patton et al., 2016).

Recently, the NCAR-LES-MLM was coupled to ozone, NO_x, HO_x, and isoprene chemistry (19 species, 41 reactions) with vertically varying photolysis rates with canopy shading and spatiotemporal variations in isoprene emissions and dry deposition with leaf area density and micrometeorology (Clifton et al., 2022). We note that our mechanism includes traditional radical recycling (i.e., via pathways that involve reaction of RO_2 and HO_2 with NO) but not more recently discovered pathways (e.g., autoxidation, which may alter the HO_x budget at low NO_x) that are difficult to represent quantitatively, even in more complex mechanisms (Bates & Jacob, 2019; Schwantes et al., 2020; Wennberg et al., 2018).

We analyze six simulations of the NCAR-LES-MLM with chemistry: three cases that perturb soil NO emissions, and two sets of the soil NO cases with different sunlight (MIDDAY and LOW_LIGHT).

- LOW_SOIL_NO has a lower bound of observed soil NO emissions (3 ppt m s^{-1}),
- BASE has an upper bound of observed soil NO emissions (15 ppt m s^{-1}), and
- VERY_HIGH_SOIL_NO has unrealistically large emissions (100 ppt m s^{-1}), but is included to advance understanding of chemistry-turbulence interactions.

In LOW_LIGHT, incoming solar radiation is 254 W m^{-2} (instead of 847 W m^{-2}) and solar zenith angle is 50.8° (instead of 18.2°). Photolysis rates are estimated offline with the NCAR Tropospheric UV and Visible Radiation Model 5.0 (Clifton et al., 2022). In general, we configure the model for weak-wind buoyancy-forced conditions. Clifton et al. (2022) detail the MIDDAY configuration. Table S1 in Supporting Information S1 details micrometeorological quantities for both sets of cases. Within the MIDDAY cases and within the LOW_LIGHT cases, the micrometeorology can be considered the same.

Simulations, excluding spin up, are ~20–40 min. Results are averaged over five turnover times corresponding to the largest and slowest eddies in the domain. The turnover time is estimated as the ABL height (z_i) divided by a velocity scale incorporating shear and buoyancy forces (w_m) (Moeng & Sullivan, 1994) (Table S1 in Supporting Information S1). Unless stated otherwise, quantities are averaged horizontally and then temporally. We only use overbars in covariances, or when the emphasis is needed to understand a quantity (e.g., in equations); in these cases, overbars represent horizontal averages, and primes represent deviations from horizontal averages. Because all variables are temporally averaged, we do not include notation denoting temporal averaging.

3. Framework for Considering Segregation Impacts on OH Reactivity

The OH reactivity (OH_r) is defined as follows:

$$OH_r = \frac{\sum_i k_i \, OH \, X_i}{OH} \tag{1}$$

The variable OH is OH concentration; X_i is concentration of reactant i ; k_i is the rate coefficient. In the absence of turbulence and any averaging, Equation 1 can simplify to $OH_r = \sum_i k_i X_i$. However, in a turbulent flow like the ABL, if we consider the average OH_r (i.e., $\overline{OH_r}$) over some time period (e.g., half an hour) and there is a non-negligible covariance between X_i and OH ("segregation") then $OH_r \neq \sum_i k_i X_i$. For example, in that case, we have:

$$\overline{OH_r} = \frac{\sum_i \overline{k_i} \, \overline{OH \, X_i}}{\overline{OH}} = \frac{\sum_i \overline{k_i} \left(\overline{OH} \, \overline{X_i} + \overline{OH' X_i'} \right)}{\overline{OH}} \tag{2}$$

(Note that because we expect k fluctuations to be small relative to reactant fluctuations, we do not examine k within the framework of segregation). To better illustrate how segregation can bias $\overline{OH_r}$, we re-write Equation 2 as:

$$\overline{OH_r} = \sum_i \overline{k_i} \, \overline{X} + \frac{\sum_i \overline{k_i} \, \overline{OH' X'}}{\overline{OH}} \tag{3}$$

The second part of Equation 3 represents the influence of segregation on $\overline{OH_r}$ from all loss reactions (the "$\overline{OH_r}$ bias").

As expected given our model configuration, we find that isoprene dominates $\overline{OH_r}$ over other reactants across our cases (Figure S1 in Supporting Information S1). Thus, we focus on the influence of OH-isoprene segregation on the $\overline{OH_r}$ bias. We note that the differences in the $\overline{OH_r}$ bias across simulations largely track the differences in OH-isoprene segregation intensities (=$\overline{OH} \, \overline{ISOP} \, / \, \overline{OH' ISOP'}$) (Figure S2 in Supporting Information S1) but the relationship is not one-to-one, due to OH differences (Figure S3 in Supporting Information S1). Segregation intensity, rather than the $\overline{OH_r}$ bias, is the quantity that typically describes segregation in the peer reviewed literature.

4. Influence of Segregation Between OH and Isoprene on OH Reactivity

Our major finding is that the $\overline{OH_r}$ bias due to OH-isoprene segregation changes substantially in sign and magnitude with height, soil NO emissions, and sunlight (Figure 1a). We describe these changes below. We first probe the MIDDAY cases, then we compare MIDDAY versus LOW_LIGHT, and finally we examine the LOW_LIGHT cases.

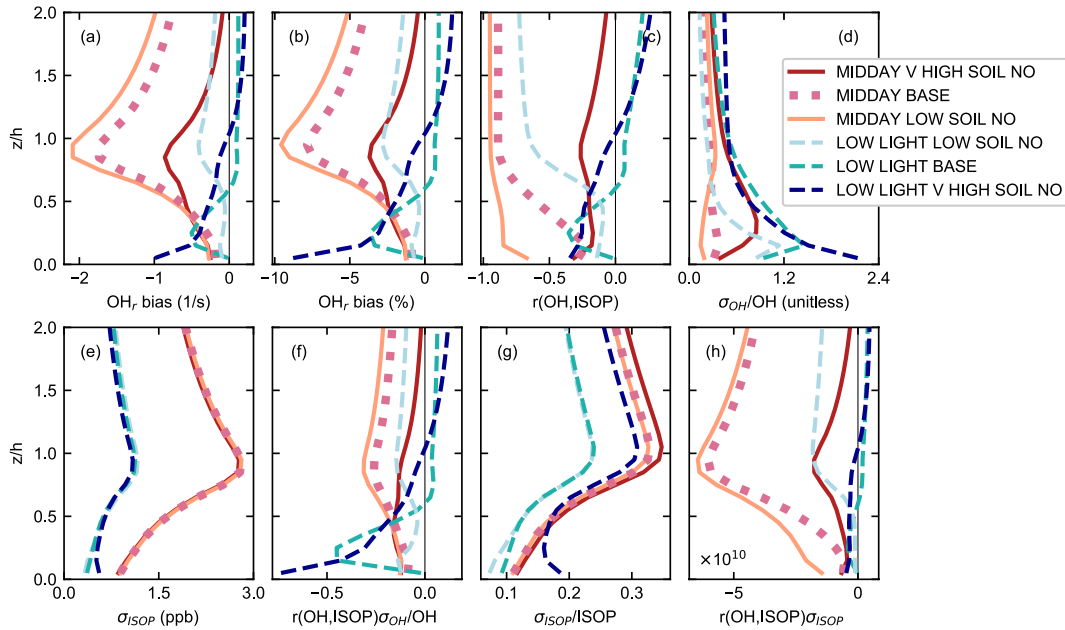

Figure 1. Vertical profiles from the canopy bottom to twofold canopy height (h) relevant to OH-isoprene segregation's influence on $\overline{OH_r}$. Panel (b) shows the percentage of $\overline{OH_r}$ that is the $\overline{OH_r}$ bias. The x-values of the data in (h) are the numbers on the x-axis multiplied by the numbers in the lower left corner.

Across the MIDDAY cases, the $\overline{OH_r}$ bias is always negative and maximizes near canopy height (h). Segregation decreases $\overline{OH_r}$ by up to 4%–9% across MIDDAY, depending on the soil NO emissions (Figure 1b). The $\overline{OH_r}$ bias is highest with lower soil NO and lowest with higher soil NO, with the largest differences above 0.5h.

To our knowledge, the role of changes in near-canopy segregation with sunlight has not been explored. We find that the absolute $\overline{OH_r}$ bias generally reduces in the LOW_LIGHT cases relative to the MIDDAY cases. However, the maximum relative impact is −9% across the LOW_LIGHT cases, which is the same as for MIDDAY. The maximum relative impact occurs for VERY_HIGH_SOIL_NO. For the lower and more realistic soil NO LOW_LIGHT cases, the relative impact ranges from −4% to +1%.

Across the LOW_LIGHT cases, segregation's impact maximizes near h for low soil NO (−3%), but maximizes in the lower canopy for higher soil NO (up to −4 to −9%). For the base case, the maximum happens around 0.25h, but for the very high soil NO case, the maximum occurs at the ground. Our finding that the height of the maximum impact changes with sunlight as well as soil NO emissions under low light conditions is new—near-canopy OH-isoprene segregation intensities have previously only been shown to be highest near h (e.g., Clifton et al., 2022; Edburg et al., 2012; Patton et al., 2001). We also find that for LOW_LIGHT, the $\overline{OH_r}$ bias is positive for high soil NO above h, and for BASE above 0.5h, but always negative for low soil NO. Positive $\overline{OH_r}$ biases are always small, but have not previously been shown to occur near the canopy for isoprene-OH segregation intensities.

5. Causes of Differences in the Influence of OH-Isoprene Segregation

Overall, we find that large changes in isoprene emissions strongly impact the OH_r bias due to OH-isoprene segregation. Tightly coupled but distinct changes in the OH-isoprene relationship versus individual OH variations that occur with changes in soil NO emissions and/or sunlight also play a key role, and drive changes in the absence of large changes in isoprene emissions. To show this, we probe the isoprene versus OH drivers of changes in the OH-isoprene covariance ($\overline{OH'ISOP'}$) among simulations via the relationship between $\overline{OH'ISOP'}$ and Pearson's correlation coefficient (r(OH, ISOP)):

$$\overline{OH'ISOP'} = r(OH, ISOP)\sigma_{OH}\,\sigma_{ISOP} \quad (4)$$

Thus, specifically, we examine how the correlation, the OH standard deviation (σ_{OH}) and the isoprene standard deviation (σ_{ISOP}) shape the covariance. Because we are interested in the impact of the covariance on $\overline{OH_r}$ (recall Equation 3), we normalize both sides of Equation 4 by $\overline{OH}$ and investigate the role of the relative OH variability ($\sigma_{OH}/\overline{OH}$) rather than absolute OH variability (σ_{OH}). We present our findings for this analysis in Section 5.1. Then, the spectral analysis in Section 5.2 offers additional insights into processes controlling the correlation. Specifically, we attempt to further understand how variability in OH and isoprene at different spatial/temporal scales contributes to the total covariance between the two chemical species.

We first present our interpretation of the results as to the processes controlling differences in the relative OH variability and OH-isoprene relationship among simulations that follows our analyses in the following subsections, in order to guide the reader. We think that relative OH variability is driven by isoprene variability under low NO, as suggested by the strong OH-isoprene anticorrelations and similar shapes of isoprene spectra and OH-isoprene co-spectra. We think that relative OH variability is driven by isoprene variability because isoprene is the major sink of OH, and in the absence of high secondary OH production, isoprene determines the nature of OH variability. (Note that we define secondary HO_x production as the sum of HO_x production chemical reaction rates in our mechanism (Table 3 of Clifton et al. (2022)), except for OH production via ozone photolysis.)

At higher NO, we think that increasing secondary HO_x production increases relative OH variability, and alters the nature of the variability, as evidenced by weakened OH-isoprene correlations. Our spectral analysis also supports this idea, showing that the OH-isoprene co-spectra become restricted to faster time scales, reflecting fast chemistry, under higher NO. There can be a positive vertical OH flux at slow time scales, presumably due to the large secondary source of OH in the canopy. We think that this vertical transport of OH with higher NO also alters the nature of the OH variability, and contributes to degrading the strong OH-isoprene anticorrelation.

We also think that the nature and magnitude of the relative OH variability are additionally influenced by the availability of sunlight (either due to time of day or canopy attenuation of radiation). We expect that the influence of sunlight on relative OH variability follows primary OH production, whereby higher primary production reduces the impact of higher secondary production. Specifically, we think that how the anticorrelation degrades relative to the corresponding increase in relative OH variability depends on availability of sunlight and thus primary OH production. Furthermore, under egregiously high NO, we think that the influence of secondary production on OH weakens due to radical burn off, and when this is coupled to downward vertical fluxes of isoprene (likely due to low isoprene and high OH), the OH-isoprene anticorrelation can be restored, at least to an extent.

5.1. Evidence From Covariance-Correlation Framework

Again, we first probe the MIDDAY cases, then we compare MIDDAY versus LOW_LIGHT, and finally we examine the LOW_LIGHT cases. Across the MIDDAY cases, the OH-isoprene correlation is negative, and weakens in strength with increases in NO (Figure 1c). The anticorrelation is very strong for MIDDAY LOW_SOIL_NO throughout the domain examined here. Relative OH variability increases with higher NO, but only inside the canopy (Figure 1d). Differences in the OH-isoprene correlation and the relative OH variability drive differences in the $\overline{OH_r}$ bias, as there are no changes in isoprene variability (Figure 1e). However, changes in the OH_r bias only occur above the lower canopy because below $0.5h$, the correlation changes buffer relative OH variability changes, leading to little $\overline{OH_r}$ bias change there (Figure 1f). On the other hand, above $0.5h$, changes in the correlation and relative OH variability are not offsetting, resulting in $\overline{OH_r}$ bias changes.

Comparing the LOW_LIGHT cases to the MIDDAY cases, isoprene variability reduces, likely due to lower isoprene abundances and emissions (Figure S2 in Supporting Information S1, Figure 1g). It is clear that the strong changes in isoprene variability with reduced sunlight have a large impact on the absolute OH_r bias. However, there are also roles for the correlation and relative OH variability in the LOW_LIGHT versus MIDDAY differences.

Ignoring LOW_LIGHT versus MIDDAY differences in the relative OH variability, differences between the sets of cases are similar to the $\overline{OH_r}$ bias (compare Figures 1a–1h), except in two instances. The first instance is that MIDDAY VERY_HIGH_SOIL_NO and LOW_LIGHT LOW_SOIL_NO are too similar for some heights above $0.5h$, but exaggerated for other heights above $0.5h$ (relative to the OH_r bias). The second instance is below $0.5h$. In these two instances, there is a role for relative OH variability. However, otherwise, our analysis suggests the correlation and isoprene variability differences together drive differences between LOW_LIGHT and MIDDAY.

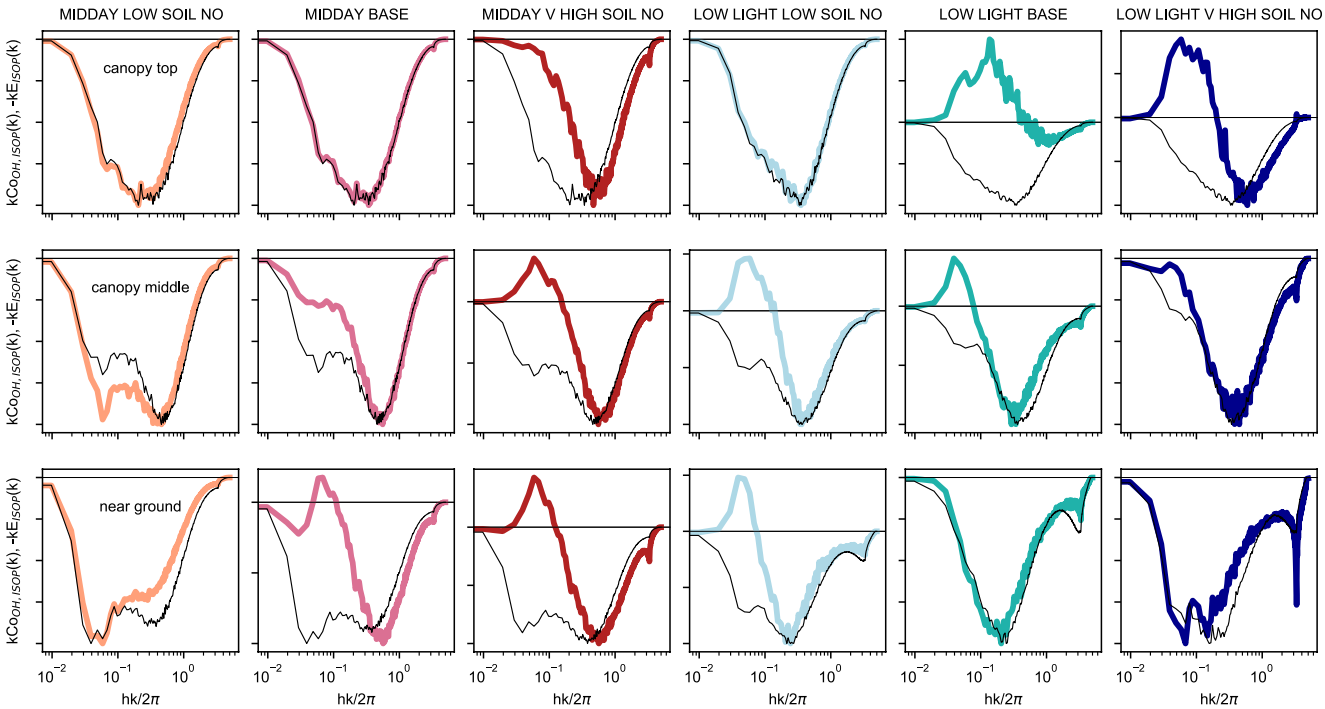

Figure 2. Azimuthally- and time-averaged two-dimensional co-spectra between OH and isoprene (colors) and spectra for isoprene (black) at three heights in the canopy. Each is normalized by its maximum positive value and multiplied by horizontal wavenumber k such that the area under the curve is proportional to the total covariance or variance. Negatives of isoprene spectra are shown to facilitate comparison with OH-isoprene co-spectra. The x-axis is such that $hk/2\pi = 1$ is the spatial scale of canopy height (h).

Across the LOW_LIGHT cases, $\overline{OH_r}$ bias differences tend to follow the correlation. One exception is that relative OH variability helps to make $\overline{OH_r}$ bias in LOW_SOIL_NO more similar to higher soil NO cases, and thus there is offsetting between changes in relative OH variability versus the correlation. In contrast to MIDDAY, the offsetting happens for all heights examined here instead of only below $0.5h$. The offsetting occurrence at all heights for LOW_LIGHT, together with the offsetting occurrence only in the lower canopy for MIDDAY, suggests that increasing NO only enhances relative OH variability under low light conditions, either due to the time of day or canopy attenuation of radiation.

5.2. Additional Evidence From Spectral Analysis and Insight Into Controlling Processes

Here we further probe the relationship between OH and isoprene by breaking down the average quantities presented in Section 5.1 by spatial/temporal scale, toward better understanding of the processes that modulate the averages. Before proceeding, we note that under the ergodic hypothesis, spatial scales are interchangeable with temporal scales (e.g., faster timescales are slower spatial scales) in this analysis, and we therefore hereinafter discuss temporal scales.

We first examine MIDDAY cases and LOW_LIGHT LOW_SOIL_NO. For these simulations, Figure 2 shows a similarity between OH-isoprene co-spectra and isoprene spectra across scales under low NO. Then, there is a decoupling between the OH-isoprene co-spectra and the isoprene spectra at slower time scales as NO increases. This behavior provides support for our hypothesis that isoprene variability controls OH variability and thus co-variability between OH and isoprene at low NO, but is not the sole driver as NO increases. The evidence for our hypothesis that secondary OH production plays a role at higher NO is that the OH-isoprene co-spectra shift to faster time scales at higher NO, which is consistent with enhanced NO accelerating the chemistry by increasing HO_x cycling (Figure S3 in Supporting Information S1).

This spectral analysis also provides clues as to other processes that may influence the OH-isoprene relationship. At some heights inside the canopy for MIDDAY higher soil NO cases and LOW_LIGHT LOW_SOIL_NO, there is a small positive covariance between OH and isoprene at slow time scales (Figure 2). This positive

OH-isoprene covariance at fast time scales happens when there are positive covariances between OH and vertical velocity (Figure S4 in Supporting Information S1) as well as between isoprene and vertical velocity (Figure S5 in Supporting Information S1), suggesting that upward transport of OH and isoprene at these scales drives their positive covariance there. So, in addition to enhanced HO_x cycling degrading the anticorrelation between OH and isoprene at higher NO, similar transport may degrade the anticorrelation as well.

In general, the story is similar for the cases discussed so far and LOW_LIGHT BASE at $0.5h$ and h as well as VERY_HIGH_SOIL_NO at h. For example, the negative OH-isoprene covariances are restricted to faster time scales with the increasing importance of secondary production and there are positive covariances at slow time scales (Figure 2). The positive covariances dominate co-spectra at h, which leads to the positive correlations observed in Figure 1c. In alignment with our thinking that this results from similar upwards vertical transport of OH and isoprene, we see that the vertical OH flux is positive at h and above for these cases (Figure S3 in Supporting Information S1).

For the LOW_LIGHT higher soil NO cases near the ground, and for LOW_LIGHT VERY_HIGH_SOIL_NO at $0.5h$, the story is different. For example, OH-isoprene co-spectra and isoprene spectra are unexpectedly very similar in shape (Figure 2). We speculate that this follows a long chain length, implying fast HO_x termination relative to HO_x cycling rate (Jaeglé et al., 2001; Martinez et al., 2003; Figure S3 in Supporting Information S1). In other words, while HO_x cycling is very fast (Figure S3 in Supporting Information S1), HO_x cycling no longer drives relative OH variability due to radical burn off, and isoprene variability can again play a role on OH and the isoprene-OH relationship. However, we think that here isoprene is not only driving variability in OH due to the fact that isoprene is a major sink of OH, because otherwise we should see similar OH-isoprene co-spectra and isoprene spectra at canopy bottom in MIDDAY VERY_HIGH_SOIL_NO where there is also a very high chain length (and we do not). Instead, we think that opposing vertical transport of isoprene and OH at most scales contributes (Figures S3 and S4 in Supporting Information S1). Positive OH fluxes in the lower canopy occur for many of the simulations, but there are only negative co-spectra between vertical velocity and isoprene at canopy bottom at most scales for LOW_LIGHT BASE and VERY_HIGH_SOIL_NO (Figure S5 in Supporting Information S1).

6. Differences in Bottom-Up Estimates and Direct Measurements of OH Reactivity Due To Segregation

There are two types of observational constraints on OH_r. The first type—bottom-up (BU) estimates—are calculated with reactant concentrations and rate coefficients (but without OH concentrations). First and foremost, we emphasize that the fidelity of BU estimates is challenged by the many OH sinks; reactants can be unknown and reactant concentrations and rate coefficients can be uncertain. Fortunately, the second type—direct measurements of OH_r—do not rely on incomplete knowledge of OH sinks (Kovacs & Brune, 2001). Comparisons between the two types of observational constraints shed light on current understanding of the contributing chemical reactions to oxidation. Inconsistencies between direct measurements and BU estimates have been reported at forests (Bsaibes et al., 2020; DiCarlo et al., 2004; Edwards et al., 2013; Hansen et al., 2014; Kaiser et al., 2016; Lew et al., 2020; Mao et al., 2012; Nölscher et al., 2012, 2016; Praplan et al., 2019; Sanchez et al., 2018; Sinha et al., 2008, 2010; Zannoni et al., 2016), as well as in the marine boundary layer (Mao et al., 2009; Thames et al., 2020; Travis et al., 2020) and some urban areas (Yang et al., 2016). For example, a recent study at a southeastern U.S. forest suggests a missing daytime OH reactivity of 5%–20% during summer 2013 (Kaiser et al., 2016).

Here we highlight how ignoring segregation in BU estimates combined with the current instrument resolution of direct measurements can create discrepancies between BU estimates and direct measurements, independent from the discrepancy created by unknown or mischaracterized OH sinks. We do this by using archived fields from our simulations at canopy top. We emphasize that, by definition, BU estimates cannot capture the segregation effect and thus can be biased due to the assumption of well-mixed conditions. For example, BU estimates assume $\overline{OH_r} = \sum_i \overline{k_i}\,\overline{X_i}$, but Equations 2 and 3 illustrate that $\overline{OH_r} \neq \sum_i \overline{k_i}\,\overline{X_i}$. We find that at the canopy top, the $\overline{OH_r}$ bias due to segregation in all reactions is −4 to −9% for MIDDAY and −3 to +1% for LOW_LIGHT, and thus the canopy-top BU estimates for our simulations would be biased this amount. In contrast, the amount of segregation that direct measurements capture depends on instrument resolution (because direct measurements do not assume $\overline{OH_r} = \sum_i \overline{k_i}\,\overline{X_i}$).

We next calculate the bias of direct measurements due to instrument resolution using archived fields from our simulations. We examine OH chemical loss to identify the impact, but the implication holds for OH_r. To sample variability generated by a turbulent eddy transporting material vertically, instrument resolution of at least half the eddy turnover time is needed, where we assume that upward and downward transport of material occurs at similar timescales. Observational analysis of passive scalar transport at a forest under similar atmospheric stability conditions (Dupont & Patton, 2012) provides support for this assumption.

Most of the variability in OH chemical loss corresponds to eddies with turnover times of 100 s or less (Figure S6 in Supporting Information S1). Thus, to capture most of the OH_r variability with a direct measurement, we infer that a resolution of at least 50 s is needed. However, the resolution of current OH_r instruments varies from 30 s to 5 min (Yang et al., 2016). We thus compare mean OH loss with mean OH loss calculated with low-pass filtering to identify whether instrument resolution biases a direct measurement due to segregation of all OH loss reactions. We find that a direct measurement with 50-s resolution would overestimate $\overline{OH_r}$ by 4%–6% for MIDDAY and either overestimate by 1% or underestimate by 0.1% for LOW_LIGHT at h. Together with the bias from ignoring segregation's effect on BU estimates, this analysis suggests that the widespread discrepancy between direct measurements and BU estimates at forests may be worse than noted previously (i.e., due to mischaracterized or unknown OH sinks), by 3%–4%.

7. Conclusion

We investigate the contribution of OH-isoprene segregation to OH reactivity inside a deciduous forest using a novel tool that resolves canopy turbulence and is coupled to simplified chemistry. While prior work already suggests that accurate estimates of the oxidation of reactive carbon inside and right above forests relies on constraints on segregation, our work shows the impact on OH reactivity and changes with sunlight (morning vs. afternoon) and soil NO emissions. OH-isoprene segregation mostly reduces OH reactivity relative to the assumption of well-mixed conditions. In morning sunlight, particularly above the canopy and with higher NO, OH-isoprene segregation can increase OH reactivity, but the impact is small.

We highlight that bottom-up estimates of OH reactivity by definition cannot incorporate segregation's effect and direct OH reactivity measurements may only consider a portion of segregation's effect, depending on instrument resolution. Accordingly, we show that the widespread discrepancy between direct measurements and bottom-up estimates ("missing OH reactivity") may be worse (up to 3%–4% at canopy top) than previously noted. We emphasize that the enhanced OH reactivity discrepancy noted here segregation falls within the uncertainty of measuring OH reactivity with the direct approach (10%–20%; Yang et al., 2016), and thus does not substantially impact the conclusions of prior work. However, as direct measurements become more accurate (e.g., Fuchs et al., 2017), and BU approaches more complete (and accurate) in terms of species concentrations and rate coefficients (e.g., Heald & Kroll, 2020; Hunter et al., 2017), segregation may become a main cause of differences between direct and BU approaches used to constrain OH reactivity.

In general, there is poor understanding of the causes of observed or simulated variability in segregation. We build mechanistic understanding of OH-isoprene segregation influences on OH reactivity by analyzing a suite of different simulations and metrics of high-frequency variations in OH and isoprene abundances as well as vertical velocities. Strong changes in isoprene emissions alter the magnitude of impact of segregation between OH and isoprene. With or without strong changes in isoprene emissions, a complex interplay of coupled OH sources and sinks influence the impact of OH-isoprene segregation on OH reactivity. High-frequency measurements of reactant and oxidant concentrations at various heights in the canopy would aid in building understanding of the environmental and chemical conditions under which segregation most strongly affects OH reactivity. Such measurements may also constrain how other more reactive volatile organic compounds (e.g., monoterpenes, sesquiterpenes) and/or other pathways of OH recycling that are not represented in our chemical mechanism alter turbulence-chemistry interactions.

Data Availability Statement

Processed data from the LES is provided in the NCAR Geoscience Data Exchange repository (https://doi.org/10.5065/m4xf-a553).

Acknowledgments
This material is based upon work supported by the National Center for Atmospheric Research, which is a major facility sponsored by the National Science Foundation under Cooperative Agreement No. 1852977. The authors acknowledge high-performance computing support from Cheyenne (https://doi.org/10.5065/D6RX99HX) provided by NCAR's Computational and Information Systems Laboratory, sponsored by NSF. S. W. was supported in part by the NOAA Cooperative Agreement with CIRES, NA17OAR4320101. The authors thank Steve Oncley for providing observed radiation profiles. The views expressed in this article are those of the authors and do not necessarily represent the views or the policies of the U.S. Environmental Protection Agency (EPA). The research presented was not performed or funded by EPA and was not subject to EPA quality system requirements.

References

Bates, K. H., & Jacob, D. J. (2019). A new model mechanism for atmospheric oxidation of isoprene: Global effects on oxidants, nitrogen oxides, organic products, and secondary organic aerosol. *Atmospheric Chemistry and Physics*, *19*(14), 9613–9640. https://doi.org/10.5194/acp-19-9613-2019

Brosse, F., Leriche, M., Mari, C., & Couvreux, F. (2018). LES study of the impact of moist thermals on the oxidative capacity of the atmosphere in southern West Africa. *Atmospheric Chemistry and Physics*, *18*(9), 6601–6624. https://doi.org/10.5194/acp-18-6601-2018

Bsaibes, S., Al Ajami, M., Mermet, K., Truong, F., Batut, S., Hecquet, C., et al. (2020). Variability of hydroxyl radical (OH) reactivity in the Landes maritime pine forest: Results from the LANDEX campaign 2017. *Atmospheric Chemistry and Physics*, *20*(3), 1277–1300. https://doi.org/10.5194/acp-20-1277-2020

Butler, T. M., Taraborrelli, D., Brühl, C., Fischer, H., Harder, H., Martinez, M., et al. (2008). Improved simulation of isoprene oxidation chemistry with the ECHAM5/MESSy chemistry-climate model: Lessons from the GABRIEL airborne field campaign. *Atmospheric Chemistry and Physics*, *8*(16), 4529–4546. https://doi.org/10.5194/acp-8-4529-2008

Carlton, A. G., Wiedinmyer, C., & Kroll, J. H. (2009). A review of Secondary Organic Aerosol (SOA) formation from isoprene. *Atmospheric Chemistry and Physics*, *9*(14), 4987–5005. https://doi.org/10.5194/acp-9-4987-2009

Chameides, W. L., Lindsay, R. W., Richardson, J., & Kiang, C. S. (1988). The role of biogenic hydrocarbons in urban photochemical smog: Atlanta as a case study. *Science*, *241*(4872), 1473–1475. https://doi.org/10.1126/science.3420404

Clifton, O. E., & Patton, E. G. (2021). Does organization in turbulence influence ozone removal by deciduous forests? *Journal of Geophysical Research: Biogeosciences*, *126*(6), e2021JG006362. https://doi.org/10.1029/2021JG006362

Clifton, O. E., Patton, E. G., Wang, S., Barth, M., Orlando, J., & Schwantes, R. H. (2022). Large eddy simulation for investigating coupled forest canopy and turbulence influences on atmospheric chemistry. *Journal of Advances in Modeling Earth Systems*, *14*(10), e2022MS003078. https://doi.org/10.1029/2022MS003078

DiCarlo, P., Brune, W. H., Martinez, M., Harder, H., Lesher, R., Ren, X., et al. (2004). Missing OH reactivity in a forest: Evidence for unknown reactive biogenic VOCs. *Science*, *304*(5671), 722–725. https://doi.org/10.1126/science.1094392

Dlugi, R., Berger, M., Zelger, M., Hofzumahaus, A., Siese, M., Holland, F., et al. (2010). Turbulent exchange and segregation of HO_x radicals and volatile organic compounds above a deciduous forest. *Atmospheric Chemistry and Physics*, *10*(13), 6215–6235. https://doi.org/10.5194/acp-10-6215-2010

Dupont, S., & Patton, E. G. (2012). Momentum and scalar transport within a vegetation canopy following atmospheric stability and seasonal canopy changes: The CHATS experiment. *Atmospheric Chemistry and Physics*, *12*(13), 5912–5935. https://doi.org/10.5194/acp-12-5913-2012

Edburg, S. L., Stock, D., Lamb, B. K., & Patton, E. G. (2012). The effect of the vertical source distribution on scalar statistics within and above a forest canopy. *Boundary-Layer Meteorology*, *142*(3), 365–382. https://doi.org/10.1007/s10546-011-9686-1

Edwards, P. M., Evans, M. J., Furneaux, K. L., Hopkins, J., Ingham, T., Jones, C., et al. (2013). OH reactivity in a south east Asian tropical rainforest during the oxidant and particle photochemical processes (OP3) project. *Atmospheric Chemistry and Physics*, *13*(18), 9497–9514. https://doi.org/10.5194/acp-13-9497-2013

Fuchs, H., Novelli, A., Rolletter, M., Hofzumahaus, A., Pfannerstill, E. Y., Kessel, S., et al. (2017). Comparison of OH reactivity measurements in the atmospheric simulation chamber SAPHIR. *Atmospheric Measurement Techniques*, *10*(10), 4023–4053. https://doi.org/10.5194/amt-10-4023-2017

Guenther, A., Hewitt, C. N., Erickson, D., Fall, R., Geron, C., Graedel, T., et al. (1995). A global model of natural volatile organic compound emissions. *Journal of Geophysical Research*, *100*(D5), 8873–8892. https://doi.org/10.1029/94JD02950

Guenther, A. B., Jiang, X., Heald, C. L., Sakulyanontvittaya, T., Duhl, T., Emmons, L. K., & Wang, X. (2012). The model of emissions of gases and aerosols from nature version 2.1 (MEGAN2.1): An extended and updated framework for modeling biogenic emissions. *Geoscientific Model Development*, *5*(6), 1471–1492. https://doi.org/10.5194/gmd-5-1471-2012

Hansen, R. F., Griffith, S. M., Dusanter, S., Rickly, P. S., Stevens, P. S., Bertman, S. B., et al. (2014). Measurements of total hydroxyl radical reactivity during CABINEX 2009 – Part 1: Field measurements. *Atmospheric Chemistry and Physics*, *14*(6), 2923–2937. https://doi.org/10.5194/acp-14-2923-2014

Heald, C. L., & Kroll, J. H. (2020). The fuel of atmospheric chemistry: Toward a complete description of reactive organic carbon. *Science Advances*, *6*, eaay8967. https://doi.org/10.1126/sciadv.aay8967

Hunter, J. F., Day, D. A., Palm, B. A., Yatavelli, R. L. N., Chan, A. W. H., Kaser, L., et al. (2017). Comprehensive characterization of atmospheric organic carbon at a forested site. *Nature Geoscience*, *10*, 748–753. https://doi.org/10.1038/NGEO3018

Jaeglé, L., Jacob, D. J., Brune, W. H., & Wennberg, P. O. (2001). Chemistry of HO_x radicals in the upper troposphere. *Atmospheric Environment*, *35*(3), 469–489. https://doi.org/10.1016/s1352-2310(00)00376-9

Kaiser, J., Skog, K. M., Baumann, K., Bertman, S. B., Brown, S. B., Brune, W. H., et al. (2016). Speciation of OH reactivity above the canopy of an isoprene-dominated forest. *Atmospheric Chemistry and Physics*, *16*(14), 9349–9359. https://doi.org/10.5194/acp-16-9349-2016

Karl, T., Guenther, A., Yokelson, R. J., Greenberg, J., Potosnak, M., Blake, D. R., & Artaxo, P. (2007). The tropical forest and fire emissions experiment: Emission, chemistry, and transport of biogenic volatile organic compounds in the lower atmosphere over Amazonia. *Journal of Geophysical Research*, *112*(D18), D18302. https://doi.org/10.1029/2007JD008539

Kaser, L., Karl, T., Yuan, B., Mauldin, R. L., Cantrell, C. A., Guenther, A. B., et al. (2015). Chemistry-turbulence interactions and mesoscale variability influence the cleansing efficiency of the atmosphere. *Geophysical Research Letters*, *42*(24), 10894–10903. https://doi.org/10.1002/2015GL066641

Kim, S.-W., Barth, M. C., & Trainer, M. (2016). Impact of turbulent mixing on isoprene chemistry. *Geophysical Research Letters*, *43*(14), 7701–7708. https://doi.org/10.1002/2016gl069752

Kovacs, T. A., & Brune, W. H. (2001). Total OH loss rate measurement. *Journal of Atmospheric Chemistry*, *39*(2), 105–122. https://doi.org/10.1023/a:1010614113786

Krol, M. C., Molemaker, M. J., & Vilà-Guerau de Arellano, J. (2000). Effects of turbulence and heterogeneous emissions on photochemically active species in the convective boundary layer. *Journal of Geophysical Research*, *105*(D5), 6871–6884. https://doi.org/10.1029/1999jd900958

Lew, M. M., Rickly, P. S., Bottoroff, B. P., Reidy, E., Sklaveniti, S., Léonardis, T., et al. (2020). OH and HO_2 radical chemistry in a midlatitude forest: Measurements and model comparisons. *Atmospheric Chemistry and Physics*, *20*(15), 9209–9230. https://doi.org/10.5194/acp-20-9209-2020

Li, D., Wang, X., Mao, J., Sheng, G., & Fu, J. (2007). Soil nitric oxide emissions from two subtropical humid forests in south China. *Journal of Geophysical Research*, *112*(D23), D23302. https://doi.org/10.1029/2007JD008680

Li, Y., Barth, M. C., Chen, G., Patton, E. G., Kim, S.-W., Wisthaler, A., et al. (2016). Large-eddy simulation of biogenic VOC chemistry during the DISCOVER-AQ 2011 campaign. *Journal of Geophysical Research: Atmospheres*, *121*(13), 8083–8105. https://doi.org/10.1002/2016JD024942

Mao, J., Ren, X., Brune, W. H., Olson, J. R., Crawford, J. H., Fried, A., et al. (2009). Airborne measurement of OH reactivity during INTEX-B. *Atmospheric Chemistry and Physics*, *9*(1), 163–173. https://doi.org/10.5194/acp-9-163-2009

Mao, J., Ren, X., Zhang, L., Van Duin, D. M., Cohen, R. C., Park, J.-H., et al. (2012). Insights into hydroxyl measurements and atmospheric oxidation in a California forest. *Atmospheric Chemistry and Physics*, *12*(17), 8009–8020. https://doi.org/10.5194/acp-12-8009-2012

Martinez, M., Harder, H., Kovacs, T. A., Simpas, J. B., Bassis, J., Lesher, R., et al. (2003). OH and HO_2 concentrations, sources, and loss rates during the Southern Oxidants Study in Nashville, Tennessee, summer 1999. *Journal of Geophysical Research*, *108*(D19), 4617. https://doi.org/10.1029/2003JD003551

Moeng, C.-H. (1984). A large-eddy-simulation model for the study of planetary boundary-layer turbulence. *Journal of the Atmospheric Sciences*, *41*(13), 2052–2062. https://doi.org/10.1175/1520-0469(1984)041<2052:alesmf>2.0.co;2

Moeng, C.-H., & Sullivan, P. P. (1994). A comparison of shear-and buoyancy-driven planetary boundary layer flows. *Journal of the Atmospheric Sciences*, *51*(7), 999–1022. https://doi.org/10.1175/1520-0469(1994)051<0999:acosab>2.0.co;2

Moeng, C.-H., & Wyngaard, J. C. (1988). Spectral analysis of large-eddy simulations of the convective boundary layer. *Journal of the Atmospheric Sciences*, *45*(23), 3573–3587. https://doi.org/10.1175/1520-0469(1988)045<3573:saoles>2.0.co;2

Nölscher, A. C., Williams, J., Sinha, V., Custer, T., Song, W., Johnson, A. M., et al. (2012). Summertime total OH reactivity measurements from boreal forest during HUMPPA-COPEC 2010. *Atmospheric Chemistry and Physics*, *12*(17), 8257–8270. https://doi.org/10.5194/acp-12-8257-2012

Nölscher, A. C., Yañez-Serrano, A. M., Wolff, S., Carioca de Araujo, A., Lavrič, J. V., Kesselmeier, J., & Williams, J. (2016). Unexpected seasonality in quantity and composition of Amazon rainforest air reactivity. *Nature Communications*, *7*(1), 10383. https://doi.org/10.1038/ncomms10383

Ouwersloot, H. G., Vilà-Guerau de Arellano, J., van Heerwaarden, C. C., Ganzeveld, L. N., Krol, M. C., & Lelieveld, J. (2011). On the segregation of chemical species in a clear boundary layer over heterogeneous land surfaces. *Atmospheric Chemistry and Physics*, *11*(20), 10681–10704. https://doi.org/10.5194/acp-11-10681-2011

Patton, E. G., Davis, K. J., Barth, M. C., & Sullivan, P. P. (2001). Decaying scalars emitted by a forest canopy: A numerical study. *Boundary-Layer Meteorology*, *100*(1), 91–129. https://doi.org/10.1023/a:1019223515444

Patton, E. G., Sullivan, P. P., Shaw, R. H., Finnigan, J. J., & Weil, J. C. (2016). Atmospheric stability influences on coupled boundary layer and canopy turbulence. *Journal of the Atmospheric Sciences*, *73*(4), 1621–1647. https://doi.org/10.1175/JAS-D-15-0068.1

Praplan, A. P., Tykkä, T., Chen, D., Boy, M., Taipale, D., Vakkari, V., et al. (2019). Long-term total OH reactivity measurements in a boreal forest. *Atmospheric Chemistry and Physics*, *19*(23), 14431–14453. https://doi.org/10.5194/acp-19-14431-2019

Sanchez, D., Jeong, D., Seco, R., Wrangham, I., Park, J.-H., Brune, W. H., et al. (2018). Intercomparison of OH and OH reactivity measurements in a high isoprene and low NO environment during the Southern Oxidant and Aerosol Study (SOAS). *Atmospheric Environment*, *174*, 227–236. https://doi.org/10.1016/j.atmosenv.2017.10.056

Schwantes, R. H., Emmons, L. K., Orlando, J. J., Barth, M. C., Tyndall, G. S., Hall, S. R., et al. (2020). Comprehensive isoprene and terpene gas-phase chemistry improves simulated surface ozone in the southeastern US. *Atmospheric Chemistry and Physics*, *20*(6), 3739–3776. https://doi.org/10.5194/acp-20-3739-2020

Sinha, V., Williams, J., Crowley, J. N., & Lelieveld, J. (2008). The comparative reactivity method – A new tool to measure total OH Reactivity in ambient air. *Atmospheric Chemistry and Physics*, *8*, 2213–2227. https://doi.org/10.5194/acp-8-2213-2008

Sinha, V., Williams, J., Lelieveld, J., Ruuskanen, R. M., Kajos, M. K., Patokoski, J., et al. (2010). OH reactivity measurements within a boreal forest: Evidence for unknown reactive emissions. *Environmental Science and Technology*, *44*(17), 6614–6620. https://doi.org/10.1021/es101780b

Sullivan, P. P., McWilliams, J. C., & Moeng, C.-H. (1996). A grid nesting method for large-eddy simulation of planetary boundary-layer flows. *Boundary-Layer Meteorology*, *80*(1–2), 167–202. https://doi.org/10.1007/bf00119016

Sullivan, P. P., & Patton, E. G. (2011). The effect of mesh resolution on convective boundary layer statistics and structures generated by large-eddy simulation. *Journal of the Atmospheric Sciences*, *68*(10), 2395–2415. https://doi.org/10.1175/jas-d-10-05010.1

Thames, A. B., Brune, W. H., Miller, D. O., Allen, H. M., Apel, E. C., Blake, D. R., et al. (2020). Missing OH reactivity in the global marine boundary layer. *Atmospheric Chemistry and Physics*, *20*(6), 4013–4029. https://doi.org/10.5194/acp-20-4013-2020

Thornton, F. C., Pier, P. A., & Valente, R. J. (1997). NO emissions from soils in the southeastern United States. *Journal of Geophysical Research*, *102*(D17), 21189–21195. https://doi.org/10.1029/97JD01567

Trainer, M., Williams, E. J., Parrish, D. D., Buhr, M. P., Allwine, E. J., Westberg, H. H., et al. (1987). Models and observations of the impact of natural hydrocarbons on rural ozone. *Nature*, *329*(6141), 705–707. https://doi.org/10.1038/329705a0

Travis, K. R., Heald, C. L., Allen, H. M., Apel, E. C., Arnold, S. R., Blake, D. R., et al. (2020). Constraining remote oxidation capacity with ATom observations. *Atmospheric Chemistry and Physics*, *20*(13), 7753–7781. https://doi.org/10.5194/acp-20-7753-2020

Wennberg, P. O., Bates, K. H., Crounse, J. D., Dodson, L. G., McVay, R. C., Mertens, L. A., et al. (2018). Gas-phase reactions of isoprene and its major oxidation products. *Chemical Reviews*, *118*(7), 3337–3390. https://doi.org/10.1021/acs.chemrev.7b00439

Williams, E. J., & Fehsenfeld, F. C. (1991). Measurement of soil nitrogen oxide emissions at three North American ecosystems. *Journal of Geophysical Research*, *96*(D1), 1033–1042. https://doi.org/10.1029/90jd01903

Yang, Y., Shao, M., Wang, X., Nölscher, A. C., Kessel, S., Guenther, A., & Williams, J. (2016). Towards a quantitative understanding of total OH reactivity: A review. *Atmospheric Environment*, *134*, 147–161. https://doi.org/10.1016/j.atmosenv.2016.03.010

Zannoni, N., Gros, V., Lanza, M., Sarda, R., Bonsang, B., Kalogridis, C., et al. (2016). OH reactivity and concentrations of biogenic volatile organic compounds in a Mediterranean forest of downy oak trees. *Atmospheric Chemistry and Physics*, *16*(3), 1619–1636. https://doi.org/10.5194/acp-16-1619-2016